

IMPROVING THE PERFORMANCE CREEP STRENGTH-ENHANCED FERRITIC STEELS

PI: Michael Santella (ORNL)

Participants:

Alstom Power (CRADA)

EPRI (Technical Affiliation)

National Institute of Materials Science (Japan)

Central Research Institute of Electric Power Industry (Japan)

BACKGROUND

Creep strength-enhanced ferritic steels such as the 9 Cr steel, ASTM A387 Grade 91, have become the key to the realization of increasingly efficient coal-fired power plants. The ability of these high-strength materials to withstand increased temperatures and pressures and/or allow the use of decreased tube wall thicknesses, at a cost that is significantly lower than that of austenitic steels of equivalent strength, is a primary reason for recent increases in the efficiency of fossil power plants worldwide. Currently, CSEF steels are used up to approximately 600°C, and are increasingly being specified and used for superheater tubing and main steam piping in coal-fired steam boilers, as well as in heat-recovery steam generators used in combined cycle gas turbine units. Until recently, the widely-held expectation was that the capabilities of CSEF steels could be pushed to 650°C (or higher), which would allow the economic use of Ni-based alloys for the higher-temperature components in planned advanced steam cycles. If this objective were realized it could eliminate the need for austenitic steels along with the problems associated with the performance of austenitic steel-to-ferritic steel weld joints.

The performance of CSEF steels, however, does not always meet expectations, and there have been reports of numerous failures of CSEF steels after only a few years in service. This practical experience apparently results from two main causes: (1) long-term properties that are not in accord with the projections made from the measurements used to qualify the alloys; and (2) an inability to attain the alloy microstructures required to achieve the desired properties in structures that have experienced certain fabrication or repair procedures. The optimum properties in CSEF steels are achieved by producing a fully-tempered martensitic microstructure through a specific normalization and tempering sequence. However, traditional welding and subsequent post-weld heat treatment (PWHT) sufficiently alters this microstructure and results in welded joints with a variety of microstructures that includes weld metal with large compositional gradients, as well as both coarse and fine-grained (FG) heat-affected zones (HAZ). The FG-HAZ regions are sources of a number of failures because the microstructures that develop there can significantly reduce creep strength. Also, the size and orientation of the FG-HAZ lead to high triaxial stress states which also accelerate creep damage. This combination results in so-called 'Type-IV' failures in CSEF steels, and studies show that the strength reduction of such joints can be on the order of 50%.

The implications of such failures include disruptions of electrical supply, increased cost of electricity, and the potential for catastrophic failure endangering the safety of power plant personnel. There is an urgent need to understand the mechanisms of failure of components made from these materials, and to devise materials solutions to improve component performance.

OBJECTIVES

The goal of this program is to improve the performance of CSEF steels, with the specific goals of providing guidelines for the maximum safe use temperatures of this class of alloys and, from understanding the causes of the current temperature limitations, developing approaches for increasing the current practical use temperature limits.

Two broad technical issues are being addressed in this effort. One relates to control of mechanical properties and microstructure, and how they depend on chemical compositions and heat treatments. The second emphasizes understanding the causes of Type IV failure and aims to develop strategies to minimize or eliminate it. The overall approach will rely on a combination of fundamental and applied studies of the effects of heat-treatment, welding, and process control on microstructural evolution and material properties.

CONTROL OF PROPERTIES AND MICROSTRUCTURE

Consideration of the importance of microstructure control in CSEF steels emphasizes the use of computational thermodynamics. CSEF steels are expected to have uniform microstructures. For instance, the microstructure of Grade 91 is typified by a matrix of tempered martensite (ferrite) that contains precipitates of chromium and alloy carbides and nitrides. For CSEF steels in general, two things are critical. Heat treating temperatures should not exceed the so-called A_1 lower critical temperature where new austenite phase can form because this will cause hard, brittle, untempered martensite to form in the alloys. Additionally, the retention of primary ferrite (stable from elevated temperatures) must be avoided because it reduces strength and ductility, and this can compromise both fabrication processes and performance in service. The maximum heat treating temperature and the probability of forming primary ferrite both depend on the specific chemical composition of a steel.

The chemical composition specification of Grade 91, for instance, may be broad enough to permit either stable high temperature ferrite to form or the critical A_1 transformation temperature to be exceeded during heat treatments. These limits are being explored for Grade 91 and similar types of steels through analysis of chemical composition specifications using computational thermodynamics. Microstructure analysis and strength testing is also being done to verify thermodynamic predictions and to confirm any unusual effects on mechanical properties. It is anticipated that this information will eventually be used to consider restrictions on ASTM-specified chemical compositions. The objective of that being more reliable, predictable use of these advanced alloys in power generation equipment. Additionally, this work could establish a basis for identifying alloy compositions with the potential for reaching service temperatures

beyond the current limits of commercial alloys. This activity represents a significant interaction with ASME Boiler and Pressure Vessel Code committees and major U.S. boiler manufacturers. It also relates to a CRADA project with Alstom Power, Inc.

RESULTS

A summary of the results from calculations of the A_1 lower critical temperature for PWHT of several CSEF steel compositions is shown in Figure 1. The analyses for estimating the variations of A_1 with composition were done using Thermo-Calc software with the Fe-DATA version 6 thermochemical database. To produce groups of alloys that spanned each specification range, five reference compositions were selected for each alloy. Then each element was varied from its minimum to its maximum while all other elements were maintained at their reference values. The 5 reference compositions were:

1. Each element set to the mid-point of its specified range
2. Austenite stabilizers (C, Co, Cu, Mn, Ni, N) set to their specified maximums; ferrite stabilizers (Cr, Mo, Nb, Si, Ta, V, W) set to their specified minimums
3. Ferrite stabilizers set to their specified maximums; austenite stabilizers set to their specified minimums
4. Each element set to the maximum specified for its range
5. Each element set to the minimum specified for its range

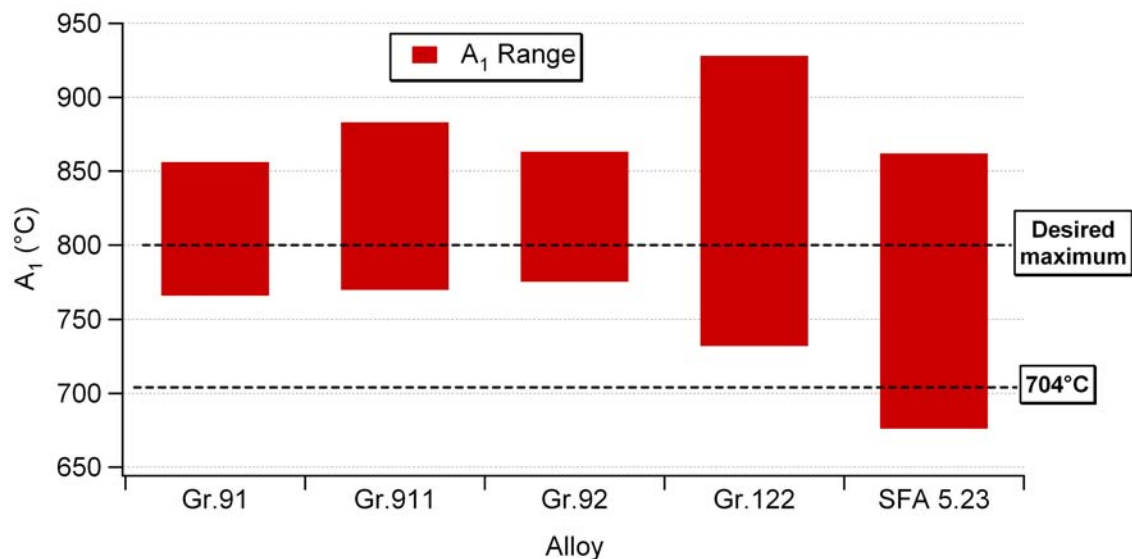


Figure 1 Graphical representation of the ranges of A_1 lower critical transformation temperatures for CSEF steel compositions

Two important temperature limits are also shown on Figure 1. One is the minimum required PWHT temperature of 704°C for the four base metal steels and one weld filler metal alloy (SFA 5.23). These alloys all conform to the material designation of P5B Group 2 meaning that according to ASME Code requirements metals within these chemical composition limits must all be post-weld heat treated using the same rules. While PWHT temperatures higher than 704°C are permitted, no maximum is specified.

Instead, it is implicitly assumed that tempering or PWHT will produce microstructures of 100% tempered martensite. The consensus of fabricators that perform PWHT for ASME Code construction is that a maximum temperature of 800°C is desirable.

The temperature limits of 704-800°C indicated on Figure 1 reveal two important concerns. The first is that setting the maximum PWHT temperature limit to 800°C permits certain alloys within the ASTM chemical composition standard specifications to be heat treated above their A_1 temperatures. The significance of this is that certain variants of these alloys that meet the chemical composition specification could actually contain untempered martensite which is the condition PWHT seeks to eliminate. The second important finding concerns the SFA 5.23 weld filler metal. In this case, not only are the A_1 temperatures of many chemical compositions permitted by its specification exceeded by setting the 800°C maximum, but the A_1 temperatures of some compositions are exceeded even at the minimum required PWHT temperature of 704°C. These results have critical implications for ASME Code construction and they are being carefully considered in deliberations to modify various requirements for the use of the steels in question.

UNDERSTANDING THE CAUSES OF TYPE IV FAILURE

The second major activity on this task emphasizes determining and understanding the effects of chemical composition and microstructure on Type IV failure in 9 Cr steels. One way this is being addressed is through basic studies to examine the underlying mechanisms that lead to this behavior. Since Type IV failure is associated with weld heat-affected zones the phase transformation behavior of 9 Cr steels under the dynamic conditions associated with welding and heat treating is being characterized.

Previous work established that phase transformation could be monitored in real-time using high-speed, high-energy x-ray diffraction at the Advanced Photon Source synchrotron. The results of initial work confirmed that the HAZ transformation behavior of an experimental 9 Cr steel known to be resistant to Type IV failure was significantly different than that of a commercial heat of Grade 92 steel. This is illustrated in Figure 2 where results of heating through a low-temperature HAZ thermal cycle are compared for Grade 92 and the experimental 9 Cr steel, N130B. Interpretation of the diffraction results indicated that the Grade 92 was heated to a peak temperature where it would have transformed almost completely to the austenite phase. The diffraction data indicate about 85% austenite formed. Cooling from that peak temperature produced a microstructure of about 60% untempered martensite, 22% new ferrite, and about 2% of retained austenite. For the N130B, the peak temperature during heating should have exceeded the temperature needed to form 100% austenite. The diffraction data indicate, however, that only about 44% austenite actually formed. On cooling, this austenite transformed to a mixture of 21% new ferrite + 23% untempered martensite.

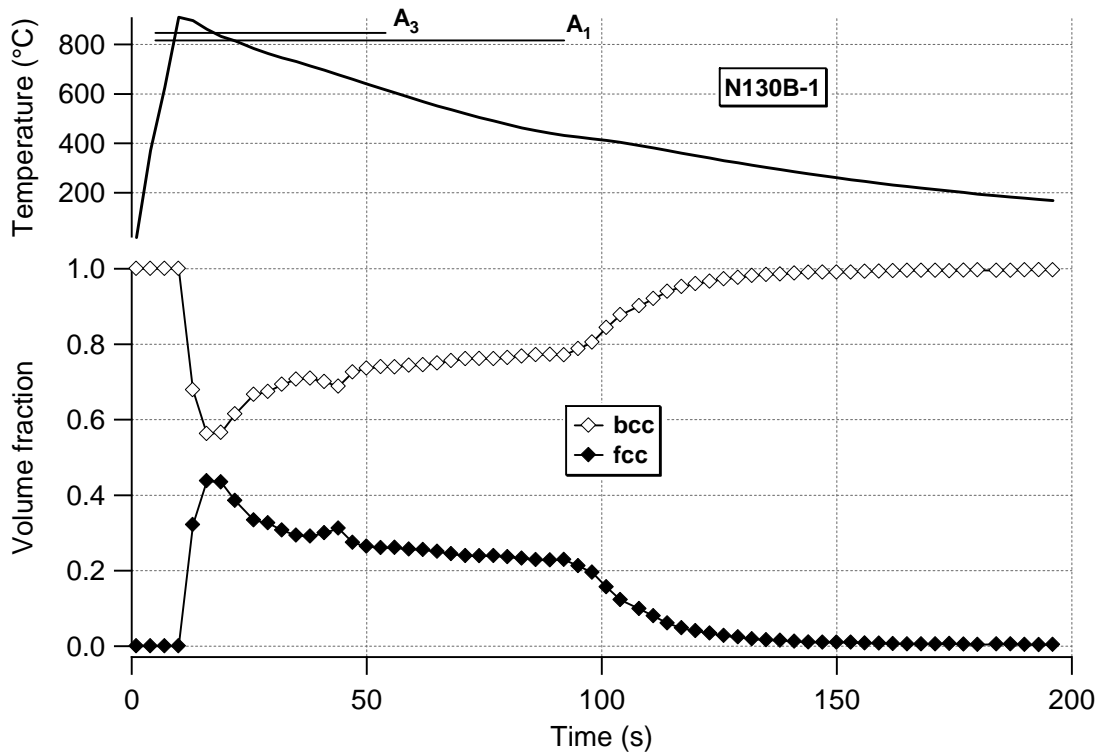
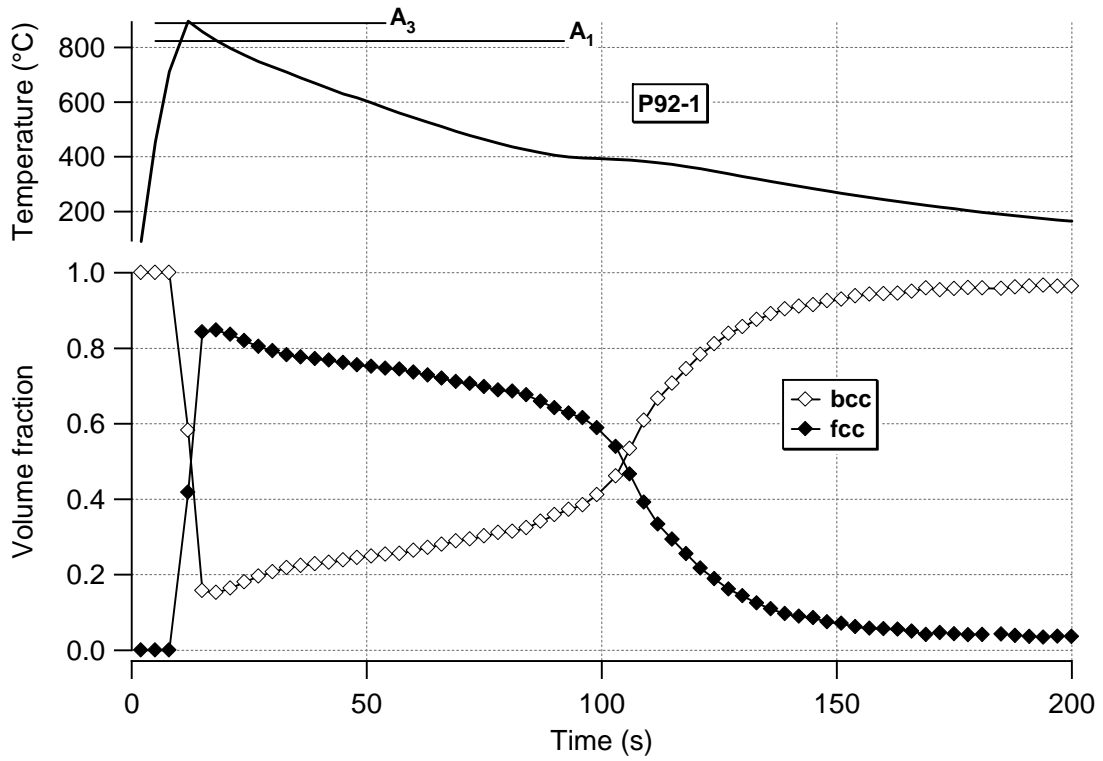


Figure 2 Synchrotron diffraction results showing the transformation behavior of Grade 92 steel (top) and the experimental 9 Cr steel N130B (bottom)

RESULTS

Current activities are aimed at associating the difference in HAZ phase transformation behavior with mechanical properties. To do this, a subsequent round of diffraction experiments was conducted. These diffraction results are currently being analyzed to confirm the differences previously observed between the Grade 92 and the experimental N130B steel. Once this is established, the specimens used for the diffraction experiments will be machined into specimens for tensile and creep testing, and subsequent microstructure characterization.

DEVELOPMENT OF NEW NICKEL-BASED ALLOYS AND WELDMENTS FOR IMPROVED CREEP-FATIGUE BEHAVIOR

To meet the target steam temperatures in future, highly-efficient power plants employing advanced ultra supercritical (A-USC) conditions, and to improve the reliability and efficiency of current fossil power systems, affordable, weldable, high-strength nickel-based alloys will be needed. Nominally solid-solution-strengthened nickel-based alloys (such as alloys 230 and 617) have the requisite creep-strength required for steam boiler and turbine temperatures up to $\sim 700^{\circ}\text{C}$, but they can suffer from creep-fatigue interactions, poor weldment strength, and involve high material cost. Age-hardenable alloys (such as alloys 263 and Inconel 740) are candidates for higher temperature (to $\sim 760^{\circ}\text{C}$), but suffer from the same drawbacks. Thus, to make the A-USC plant more economically competitive and to improve its reliability, there is a need for lower-cost nickel-based alloys with improved creep-fatigue and weldment performance.

The baseline behavior which the new alloy developments must exceed is being set by a study involving researchers at ORNL and the Central Research Institute of the Electric Power Industry (CRIEPI) in Japan. This study was formalized by a memorandum of agreement between ORNL and CRIEPI which initiated a joint program to develop the baseline creep, fatigue, and creep-fatigue behavior of thick-section alloy 263. Fatigue and creep-fatigue tests are being conducted at ORNL and the data are being analyzed by CRIEPI. A staff scientist from CRIEPI was on sabbatical at ORNL to jointly perform the initial experiments.

RESULTS

To better understand some of the complexities of creep-fatigue interactions, the following alloy 263 specimens were prepared: (1) aged at 750°C for 216 h; (2) creep tested at conditions of 750°C , 180MPa, life of 3013 h; (3) fatigue tested at 750°C , $\Delta\varepsilon = 0.7\%$, life of 2070 cycles, and (4) creep-fatigue tested at 750°C , $\Delta\varepsilon = 0.7\%$, tensile hold 6 min, life of 737 cycles. A longitudinal cross section was machined from each specimen and examined by electron backscatter diffraction in a scanning electron microscope. Figure 3 shows the local orientation spread (LOS) maps for the four specimens. The appearance of the microstructure in Figure 3(a) indicates that there was no significant local strain near grain boundaries as expected. There is a macroscopic fatigue crack at a grain boundary in the lower middle part of Figure 3(b), and a highly deformed zone extending in advance

of the crack is evident. In comparison to the fatigue-tested specimen, the wide spread of blue-to-green zones inside the grains of the creep-tested specimen, Figure 3(c), indicates that the inhomogeneous constraint from the surrounding grains caused an uneven creep deformation in each grain. The creep-fatigue specimen, Figure 3(d) also shows an uneven distribution of LOS. However, unlike the creep condition, local deformation also tended to concentrate near the grain boundaries. Only in the creep-fatigue case are LOS changes greater than 15 degrees observed within about 15 μm of the grain boundaries. This distinctive trend is considered to be the result of microscopically irreversible accumulation of deformation due to dislocations pile-ups induced in the fatigue period. Additional investigations are continuing to clarify the creep-fatigue damage mechanism for this material.

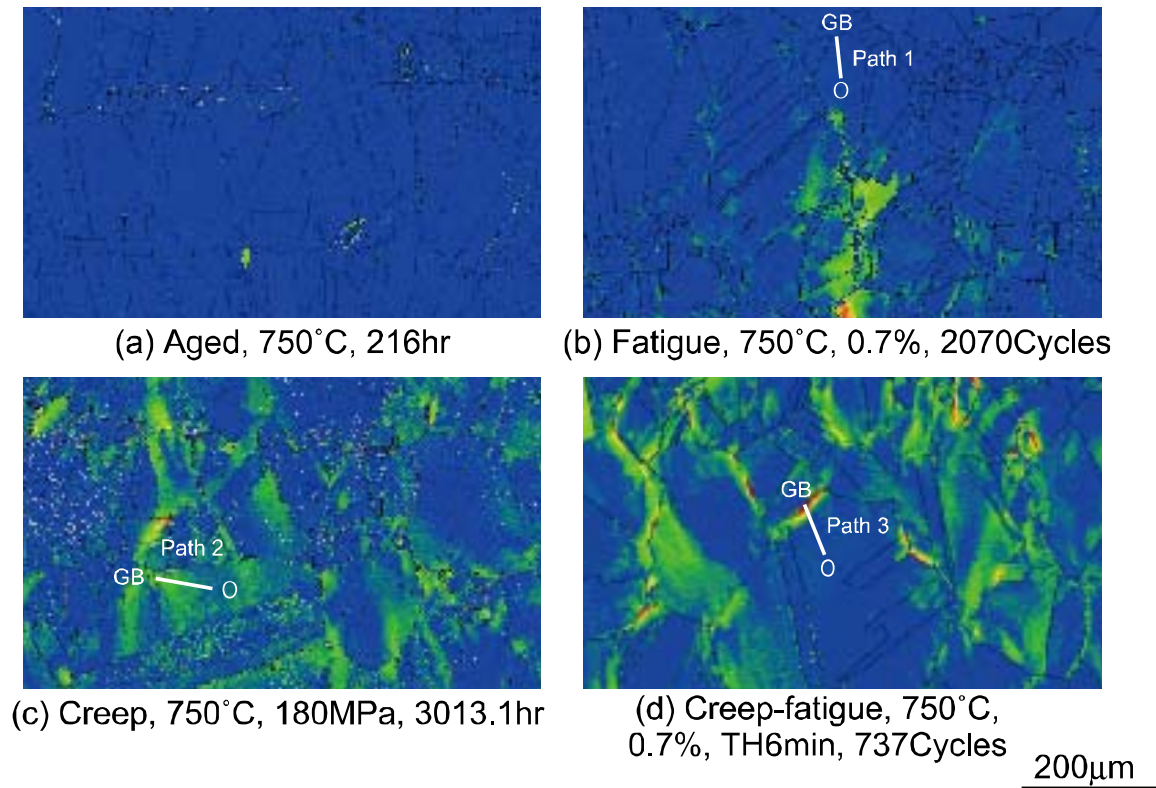


Figure 3 Electron backscatter diffraction image of local orientation spread in alloy 263 for conditions of (a) aged, (b) fatigue tested, (c) creep tested, and (d) creep-fatigue tested